Journal of Biomolecular NMR (2005) 32: 23–30
DOI 10.1007/s10858-005-3592-0

Article

Sensitivity enhancement in NMR of macromolecules by application of optimal control theory

Dominique P. Frueh[a], Takuhiro Ito[b], Jr-Shin Li[c], Gerhard Wagner[a], Steffen J. Glaser[d] & Navin Khaneja[c,*]

[a]*Department of Biological Chemistry and Molecular Pharmacology, Harvard Medical School, Boston, MA, 02115;* [b]*RIKEN Genomic Sciences Center, 1-7-22 Suehiro-cho, Tsurumi, Yokohama, 230-0045Japan;* [c]*Division of Engineering and Applied Sciences, Harvard University, Cambridge, MA, 02138;* [d]*Department of Chemistry, Technische Universität München, 85747 Garching, Germany*

Received 6 December 2004; Accepted 16 February 2005

Key words: cross-correlation, GroEL, optimal control, macromolecular NMR, relaxation

Abstract

NMR of macromolecules is limited by large transverse relaxation rates. In practice, this results in low efficiency of coherence transfer steps in multidimensional NMR experiments, leading to poor sensitivity and long acquisition times. The efficiency of coherence transfer can be maximized by design of relaxation optimized pulse sequences using tools from optimal control theory. In this paper, we demonstrate that this approach can be adopted for studies of large biological systems, such as the 800 kDa chaperone GroEL. For this system, the ^{1}H–^{15}N coherence transfer module presented here yields an average sensitivity enhancement of 20–25% for cross-correlated relaxation induced polarization transfer (CRIPT) experiments.

Abbreviations: CSA – Chemical Shift Anisotropy; CRIPT – Cross-Relaxation Induced Polarization Transfer; SQC – Single Quantum Coherence; TROPIC – Transverse Relaxation Optimized Polarization transfer Induced by Cross-correlation effects.

Introduction

Nuclear Magnetic Resonance (NMR) is a widely used technique for structural, kinetic and dynamic studies of biological molecules (Ferentz and Wagner, 2000; Abelson and Simon, 2001). Application of NMR to very large macromolecular systems is limited, however, by the low sensitivity of the technique, rapid transverse relaxation and spectral crowding. Important technological developments, such as cryogenic probes, high-field magnets, or advanced pulse sequences have alleviated some of these problems. However, there is a fundamental limitation of NMR spectroscopy with very large systems because transverse relaxation is enhanced with increasing molecular size. This leads to rapid decay of signals during and after pulse sequences applied to derive structural information. In particular, transverse relaxation leads to poor efficiency of coherence transfer in multidimensional NMR experiments. In contrast to transverse spin order, relaxation of longitudinal spin order components decreases with increasing molecular size, a phenomenon we want to take advantage of for the design of coherence transfer modules described in this manuscript.

The goal of the work described here is to utilize the slow longitudinal relaxation to improve the

*To whom correspondence should be addressed. E-mail: navin@hrl.harvard.edu

sensitivity of multiple-resonance experiments. We can significantly improve efficiency of coherence transfer by storing spin order as much as possible in its slowly relaxing longitudinal components. The experiment described here is based on recently developed concepts of relaxation optimized pulse sequences designed using optimal control theory (Khaneja et al., 2003a, b, 2004). We consider two-dimensional experiments that correlate the signals of two atoms that are covalently bound, e.g. an amide proton and its corresponding nitrogen atom. In the standard HSQC (Heteronuclear Single-Quantum Correlation spectroscopy) experiment (Bodenhausen and Ruben, 1980), this is achieved by transferring the magnetization from a proton to its attached nitrogen via the scalar coupling between the two spins. However, even for this simple experiment, the size of the molecules that can be studied is greatly limited by transverse relaxation. This effect leads to a decay of the signal over the course of the experiment, sometimes to the extent that no signal can be detected. Major improvements have been made in reducing these losses by using interference effects (or cross-correlated relaxation) between relaxation mechanisms involving the chemical shift anisotropy (CSA) of one spin and the dipole–dipole interaction (DD) of that spin with a nearby, second spin. Cross-correlated relaxation slows the decay of the signal during encoding and detection periods as is exploited in Transverse Relaxation Optimized Spectroscopy (TROSY) (Pervushin et al., 1997). Moreover, the interference between ^{1}H proton CSA and amide proton–nitrogen ^{1}H–^{15}N DD can be used to transfer magnetization from proton to nitrogen (Brüschweiler and Ernst, 1991; Dalvit, 1992)

$$\mathrm{H}_x \xrightarrow{R_{\mathrm{H/HN}}^{\mathrm{CSA/DD}}} -2\mathrm{H}_x\mathrm{N}_z \qquad (1)$$

where $R_{\mathrm{H/HN}}^{\mathrm{CSA/DD}}$ is the relevant cross-correlation rate, acting on the single-quantum coherence (SQC) H_x. The efficiency of this transfer depends on the ratio of the cross-correlation rate to the autorelaxation rate and is largely independent of the size of the molecule (Riek et al., 1999). Thus, in the case of large systems, scalar couplings are supplemented or even supplanted by cross-correlated relaxation to achieve magnetization transfer in, respectively, the CRINEPT (Cross-correlated Relaxation Enhanced Polarization Transfer) (Riek et al., 1999) and CRIPT (Cross-Relaxation Induced Polarization Transfer) experiments (Brüschweiler and Ernst, 1991). In spite of these improvements, until recently the maximum transfer efficiency for a molecule with given relaxation rates was unknown, and no experiment had been designed that would achieve such a maximum transfer (Khaneja et al., 2003a). In this publication, we make use of optimal control theory to maximize the efficiency of coherence transfers mediated solely by cross-correlation effects. We illustrate the method by recording proton nitrogen correlation maps of the 800 kDa homotetradecameric protein GroEL. This protein was previously investigated by Wüthrich and coworkers by using the [^{15}N, ^{1}H]-CRIPT-TROSY experiment (Riek et al., 2002), which we take as a reference. We show that the technique presented here enhances coherence transfer efficiency by 20–25% when compared to the best and optimized pre-existing CRIPT coherence transfer method.

Material and methods

In the reference CRIPT experiment shown in Figure 1c (Brüschweiler and Ernst, 1991; Riek et al., 2002), the transfer depicted in Equation (1) is achieved by applying a 90° pulse on proton frequencies followed by a mixing time T_{C}. The evolution under chemical shifts and scalar couplings is refocused during the mixing time. The anti-phase term $2\mathrm{H}_x\mathrm{N}_z$ resulting from cross-correlated relaxation is then converted into longitudinal two-spin order $2\mathrm{H}_z\mathrm{N}_z$. The efficiency of the transfer is usually optimized by adjusting T_{C}, based on the ratio of the cross-correlation rate to the transverse auto-relaxation rate. Recently developed methods relying on optimal control theory exploit the fact that the relaxation rates of longitudinal operators H_z and $2\mathrm{H}_z\mathrm{N}_z$ are much smaller than those of the transverse operators H_x and $2\mathrm{H}_x\mathrm{N}_z$. Thus, storing part of the spin order in a longitudinal state can further minimize signal losses during the transfer pulse sequence module. The resulting relaxation optimized experiment involves gradual rotation of the magnetization from H_z to H_x, where the latter is converted to $-2\mathrm{H}_x\mathrm{N}_z$ through cross-correlated relaxation. For an isolated spin system, this can be achieved by using a selective pulse applied on-resonance with the unique proton frequency. Throughout the

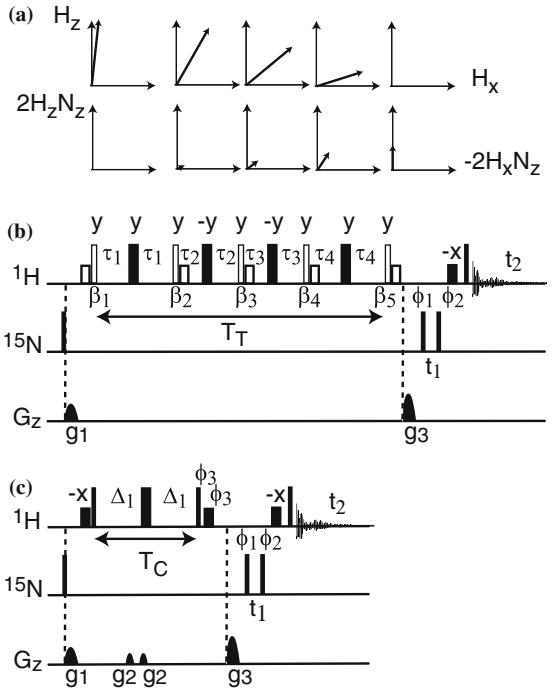

Figure 1. (a) Evolution of the source density operator elements H_x and H_z (top) and the target terms, $-2H_xN_z$ and $2H_zN_z$ (bottom). The lengths and orientations of the vectors were simulated for a transfer optimized for rates with magnitudes $R_2(H_x) = 446\ s^{-1}$ and $R_{H/HN}^{CSA/DD}(H_x) = 326\ s^{-1}$. (b) Pulse sequence obtained with optimal control theory. Narrow and large black rectangles indicate 90 and 180° pulses, respectively. Small solid rectangles indicate 90° rectangular water selective pulses of length 600 μs with a bandwidth of 0.55 ppm (416.6 Hz). Narrow open rectangles represent hard pulses with flip angles β_i and small broad open rectangles indicate water selective pulses with the same flip angles β_i but with an opposite phase, −y. For a transfer optimized for the rates given above, $\beta_1 = 18.4°$, $\beta_2 = 22.3°$, $\beta_3 = 23.5°$, $\beta_4 = 22.2°$, and $\beta_5 = 18.3°$. The corresponding delays are $\tau_1 = 0.3511$ ms, $\tau_2 = 0.2594$, $\tau_3 = 0.2595$ ms, and $\tau_4 = 0.3525$ ms with a total $T_T = 2.44$ ms. ϕ_1 = x, −x; ϕ_2 = 4(x), 4(−x); ϕ_{rec} = −x, x, −x, x, x, −x, x, −x. The power of the flip-back pulses were adjusted experimentally leading to the following values of the flip angles: 20.4°, 19.6°, 23.2°, 21.9° and 22.8°, respectively for β_1 to β_5. (c) CRIPT pulse sequence (Riek et al., 2002) $\Delta_1 = 0.455$ ms for the rates mentioned above, $T_C = 0.91$ ms. ϕ_3 = 2(x), 2(−x); ϕ_{rec} = −x, x, x, −x, x, −x, −x, x. Phase sensitivity was achieved by applying the States-TPPI technique to phase ϕ_1. A second pair of experiments were recorded for the rates $R_2(H_x) = 578\ s^{-1}$ and $R_{H/HN}^{CSA/DD}(H_x) = 422\ s^{-1}$: T_T = 1.66 ms ($\tau_1 = 0.2718$ ms, $\tau_2 = 0.1918$ ms, $\tau_3 = 0.1726$ ms, and $\tau_4 = 0.1916$ ms), $\beta_1 = 23.4°$, $\beta_2 = 28.8°$, $\beta_3 = 31.5°$, $\beta_4 = 31.5°$, and $\beta_5 = 41.4°$. The length of the flip-back pulse had to be reduced to 450 μs, corresponding to a bandwidth of 0.74 ppm (555.5 Hz). The values of the flip-angles of the flip-back pulses were adjusted experimentally to 24.9°, 24.4°, 29.9°, 29.9° and 49.5°, respectively for β_1 to β_5; $T_C = 0.7$ ms, Δ_1 = 0.35 ms.

optimal transfer process the ratio of the expectation values of the two transverse operators is maintained constant to a value that depends on their relaxation rates (Khaneja et al., 2003a):

$$\frac{\langle -2H_xN_z\rangle}{\langle H_x\rangle} = \eta, \tag{2}$$

where $\eta = \xi - \sqrt{\xi^2 - 1}$, with

$$\xi = \frac{R_2(H_x)}{R_{H/HN}^{CSA/DD}(H_x)}, \tag{3}$$

and $R_2(H_x)$ and $R_{H/HN}^{CSA/DD}(H_x)$ are the auto- and cross-correlated relaxation rates, respectively, affecting the proton SQC. This transfer technique can be made broadband by discretely flipping the magnetization toward the transverse plane. This is achieved by successive application of hard radio-frequency pulses with small flip angles separated by delays and refocusing pulses during which the in-phase coherence is converted to the desired anti-phase coherence (Khaneja et al., 2004). The resulting experiment then is comprised of n evolution periods ($n = 4$ in the current experiment) where each small flip angle pulse simultaneously flips proton magnetization toward the transverse plane and the antiphase component toward the longitudinal axis. The flip angles and the lengths of the evolution periods can be determined based on methods of dynamic programming in subject of optimal control (Khaneja et al., 2004). A 180° pulse on protons in the center of each evolution period refocuses evolution under chemical shifts and scalar couplings. We refer to this new experiment as TROPIC (Transverse Relaxation Optimized Polarization transfer Induced by Cross-correlation effects). Computation of the flip angles and lengths of the evolution periods for the TROPIC experiment is discussed in detail in the Supporting material. The program for computing TROPIC pulse sequence can be downloaded from the website 'http://eecs.harvard.edu/∼ shin'. The optimal number of evolution periods can be estimated through simulation. When $n = 1$, no relaxation optimization is obtained and the experiment is identical to the original CRIPT technique. When the transverse period is subdivided into periods where the magnetization is only partially oriented toward the transverse plane, relaxation losses decrease. For the current case, with the rates $R_2(H_x) = 446\ s^{-1}$

and $R_{H/HN}^{CSA/DD}(H_x) = 326\ s^{-1}$ (see below), the theoretical improvement over the standard CRIPT experiment is 10% for $n = 2$, 17% for $n = 3$, 21% for $n = 4$ and 22% for $n = 5$. Although the maximum improvement would be obtained with an infinite number of subperiods, in practice, finite pulse durations and imperfections deteriorate this improvement when increasing the value of n. As the number of evolution periods increases, so does the number of refocusing pulses. Since each 180° pulse has non-zero duration in which the magnetization passes through the transverse plane, an increased number of such pulses contributes to relaxation losses. In general, there is an optimal number of evolution periods for given relaxation rates, which can be readily determined by simulations. In the current case, no substantial gain is obtained when increasing n from 4 to 5. In addition, four evolution periods allow for incorporation of a supercycle on the 180° refocusing pulses. The [^{15}N, ^{1}H]-TROPIC-TROSY pulse sequence resulting from optimal control theory (see above) is displayed in Figure 1b. During the period T_T, the proton magnetization H_z is slowly flipped toward the transverse plane, where the single-quantum coherence H_x can be converted into anti-phase coherence $-2H_xN_z$. This is accomplished by dividing the total period T_T in four periods of lengths $2\tau_i$ in which hard pulses with small flip angles β_i (denoted by narrow open rectangles labeled with the corresponding flip angles β_i) are used to control the orientation of the magnetization. The generated term is concomitantly stored as longitudinal two-spin order $2H_zN_z$. This is achieved by calculating the values of the delays τ_i and the flip angles β_i for a given set of the relaxation rates $R_2(H_x)$ and $R_{H/HN}^{CSA/DD}(H_x)$, which were estimated as described below. A simulation of the magnetization transfer for a given set of relaxation rates is depicted in Figure 1a. After a transfer period of total length T_R, a z-filter is applied to suppress unwanted coherences once all proton magnetization has been converted to longitudinal two-spin order. Following a 90° pulse, indicated by a solid rectangle, nitrogen SQC is allowed to evolve during the encoding time t_1. Finally, the anti-phase proton SQC $2H_xN_z$ is detected. For comparison, the pulse sequence of [^{15}N, ^{1}H]-CRIPT-TROSY as used in Riek et al. (2002) is displayed in Figure 1c with the same scale as in Figure 1b. As mentioned in Riek et al. (2002) particular care must be taken to ensure that the water is maintained along the z-axis during experiments to avoid cross-saturation between water and amide proton spins. For the [^{15}N, ^{1}H]-TROPIC-TROSY the water flip-back pulse (Grzesiek and Bax, 1993) lengths were calculated in order to compensate the small flip angles of each accompanying hard pulse. Thus, five water-selective pulses with flip angles β_i and phases opposing the phases of the accompanying hard pulses were inserted in the period T_T. These pulses are denoted by broad open rectangles in Figure 1b. In both experiments, each water-selective pulse was then adjusted individually, not only to minimize the residual signal of water protons, but also simultaneously to maximize the signals of the protein. To design the experiments, the relaxation rates $R_2(H_x)$ and $R_{H/HN}^{CSA/DD}(H_x)$ were first estimated assuming a rigid molecule (see for example Goldman, 1984; Boyd et al., 1991; Brüschweiler and Ernst, 1991; Cavanagh et al., 1996) including dipolar interactions with remote protons and using the proton CSA as determined by Bax and Cornilescu (2000). This enables the estimation of the ratio ξ. The transfer in the CRIPT experiment was then optimized by changing the delay T_C as described in Riek et al. (2002), while focusing on signals with small intensities. The relaxation rates corresponding to an optimum transfer with that delay were then calculated by using

$$R_{H/HN}^{CSA/DD}(H_x) = \frac{\coth^{-1}(\xi)}{\pi T_C} \tag{4}$$

and $R_2(H_x)$ was deduced from Equation (3). Finally, these values were used to generate the corresponding TROPIC experiment.

^{2}H, ^{15}N-labeled GroEL was over-expressed in *E. coli* BL21 strain transformed by the plasmid pG-Tf3 (Nishihara et al., 2000) using M9 media enriched with $^{15}NH_4Cl$ and $^{2}H_2O$. The over-expressed protein was purified with Q sepharose Fast Flow anion exchange and HiLoad 16/60 superdex 200 gel filtration column chromatographies (Amersham Biosciences). The protein was concentrated to a final concentration of 0.08 mM (1.1 mM per monomer) at pH = 6.0 with 25 mM potassium phosphate and 20 mM KCl.

Each spectrum was obtained in 17 h by recording 72×1024 complex points in ^{15}N and ^{1}H dimensions, respectively (1024 scans, 0.3 s recy-

cling delay). The spectral widths were 16.033 ppm for ^{1}H and 35 ppm for ^{15}N. The measurements were effected at 35° on a Bruker 750 MHz AVANCE spectrometer equipped with a quadruple resonance probe. The spectra were processed as described in Riek et al. (2002).

Results and discussion

We first recorded a pair of CRIPT and TROPIC experiments with T_C = 0.9 ms and T_T = 2.4 ms, respectively. The CRIPT transfer time had been chosen to be shorter than in the experiment of Riek et al. (2002) (where T_C = 1.4 ms) since the focus here was on signals with large relaxation rates. The resulting spectra are displayed in Figure 2a (CRIPT) and b (TROPIC). Signals with slow relaxation rates, such as those of residues located in loops or those of side-chains, are far from the optimized conditions and will not be discussed in the analysis of the results. They appear as strong antiphase signals, since the experiments detect proton SQC in antiphase with nitrogen. For less mobile protons the negative component of the antiphase doublet is broadened beyond detection due to its relaxation, which is enhanced by the CSA/DD cross-correlation effect. A number of peaks corresponding to these more rigid residues appear in the TROPIC spectrum due to the predicted enhancement (see circled peaks in Figure 2b). However, the enhancement is far from being uniform. The magnitude of the relaxation rates involved in both types of transfers is expected to vary from residue to residue, so that a non-uniform enhancement will be observed. The cross-correlation rate depends on the magnitude of the proton CSA tensor and on its orientation with respect to the dipole–dipole interaction (Goldman, 1984; Boyd et al., 1991). In addition, internal motions occurring on a time scale which is faster than the tumbling of the molecule affect relaxation rates, especially if these motions are anisotropic (Fischer et al., 1997; Brutscher et al., 1998; Lienin et al., 1998; Frueh, 2002). Both auto- and cross-correlated relaxation rates also vary with the orientation of each interaction vector with respect to the axes of the rotational diffusion tensor of the molecule (Woessner, 1962; Brüschweiler et al., 1995). Conformational exchange and chemical exchange will affect the detected signals by enhancing the magnitude of the autorelaxation rate and possibly affecting the cross-correlation rate. To determine the effect of all of these variations, we simulated the

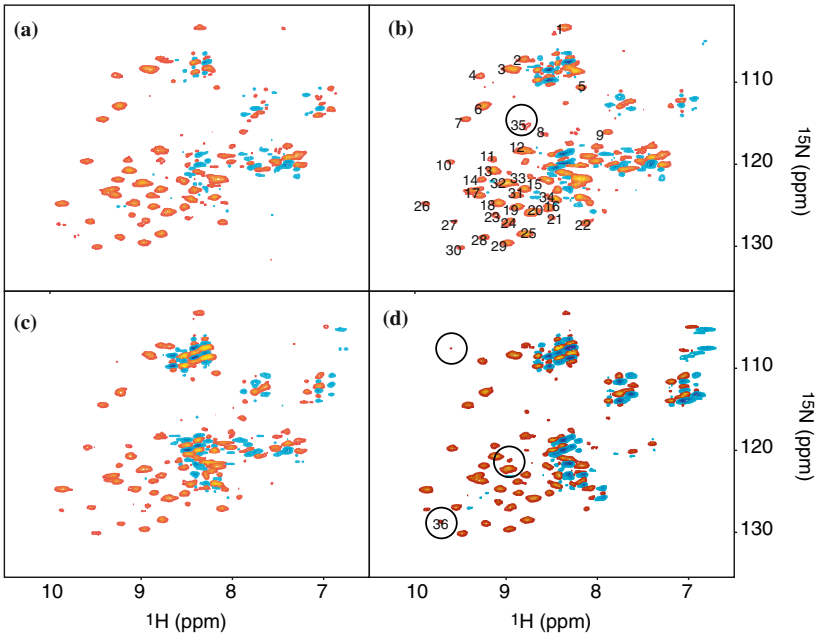

Figure 2. TROPIC (b and d) and CRIPT (a and c) spectra of GroEL recorded with T_C = 0.91 ms (a), T_T = 2.44 ms (b), T_C = 0.7 ms (c), and T_T = 1.66 ms (d).

conversion of magnetization during a transfer period optimized for given values of the auto- and cross-correlation rates, $R_2(\mathrm{H}_x) = 446\ \mathrm{s}^{-1}$ and $R_{\mathrm{H/HN}}^{\mathrm{CSA/DD}}(\mathrm{H}_x) = 326\ \mathrm{s}^{-1}$ with the resulting ratio $\xi^{-1} = 0.73$. The relaxation rates were then varied to measure the change of efficiency of both experiments under non nominal conditions. The results of these simulations are illustrated in Figure 3. Each curve in Figure 3a corresponds to a fixed ratio of the two rates while their magnitude is changed, with the solid lines depicting the case $\xi^{-1} = 0.73$ for which the pulse sequence was optimized. As expected, the yield is reduced for both experiments when the conditions are away from the nominal case. The ratio of the efficiencies of the TROPIC to CRIPT experiments (Figure 3b) shows that the enhancement is increased as the rates deviate together from the optimal conditions. Thus, even if both experiments suffer losses when the rates are different from the values used to optimize the transfer, smaller losses are found in the TROPIC experiment.

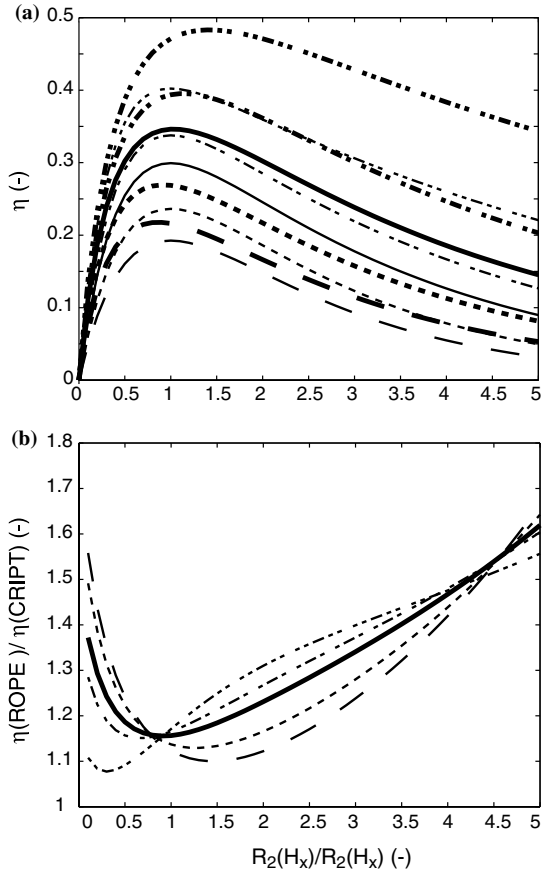

Figure 3. (a) Simulations of the transfer yields (η) of the TROPIC (thick lines) and CRIPT (thin lines) transfers in experiments optimized for the rates $R_2(\mathrm{H}_x) = 446\ \mathrm{s}^{-1}$ and $R_{\mathrm{H/HN}}^{\mathrm{CSA/DD}}(\mathrm{H}_x) = 326\ \mathrm{s}^{-1}$ ($T_{\mathrm{C}} = 0.91$ ms, $T_{\mathrm{T}} = 2.44$ ms). The efficiency was calculated as a function of the change in magnitudes of both the cross-correlation rate and the autorelaxation rate from their nominal value, denoted by $R_2^0(\mathrm{H}_x)$ for the latter. The simulations were effected for various values of the fixed ratio $\xi^{-1} = 0.5$ (dashed line), 0.6 (doted line), 0.7 (nominal value, solid line), 0.8 (dashed and dotted) and 0.9 (dash – two dots). (b) Ratio of the curves obtained in (a) to compare the robustness of the two types of experiments.

Under optimal conditions, i.e., when $R_2(\mathrm{H}_x) = R_2^0(\mathrm{H}_x)$, the gain is calculated to be around 21%. This simulation was repeated for four values of the ratio of the two relaxation rates. When this ratio is different than the nominal value, the gain in efficiency of TROPIC over CRIPT may reduce. The predicted robustness of the TROPIC experiment suggests that it may be beneficial to optimize the sequence for fast relaxing signals. Losses for residues with smaller relaxation rates will affect signals of larger intensities. As shown above, these losses are expected to be smaller in the TROPIC experiment than in the CRIPT experiment. Thus, we repeated the two experiments with transfer times of $T_{\mathrm{C}} = 0.7$ ms and $T_{\mathrm{T}} = 1.66$ ms, i.e., for a transfer optimum for signals with large relaxation rates. The resulting spectra are shown in Figure 2c and d. A few peaks are now emerging in the TROPIC spectrum and low intensity peaks are enhanced while most other peaks are little affected. No new peaks are observed in the CRIPT spectrum. This suggests that these signals can be detected because the transfer is more efficient in the TROPIC experiment for relaxation rates that are different than those the experiments were optimized for. The signal enhancement is best seen in the traces shown in Figure 4a, particularly peak 35 which is absent in the two CRIPT experiments and peak 36, which barely emerges from the noise in the CRIPT spectra. The intensities of 34 peaks uniformly distributed in the spectrum were measured. Other signals that were too close to the noise in the CRIPT experiment (such as peaks 35 and 36) or which were near large antiphase signals belonging to slow relaxing residues were discarded. The ratio of the TROPIC signal intensities to the CRIPT signal intensities are shown in Figure 4b ($T_{\mathrm{C}} = 0.9$ ms and $T_{\mathrm{T}} = 2.4$ ms) and c ($T_{\mathrm{C}} = 0.7$ ms and $T_{\mathrm{T}} = 1.6$ ms). In both pairs of experiments, a few signals are actually decreased in the TROPIC

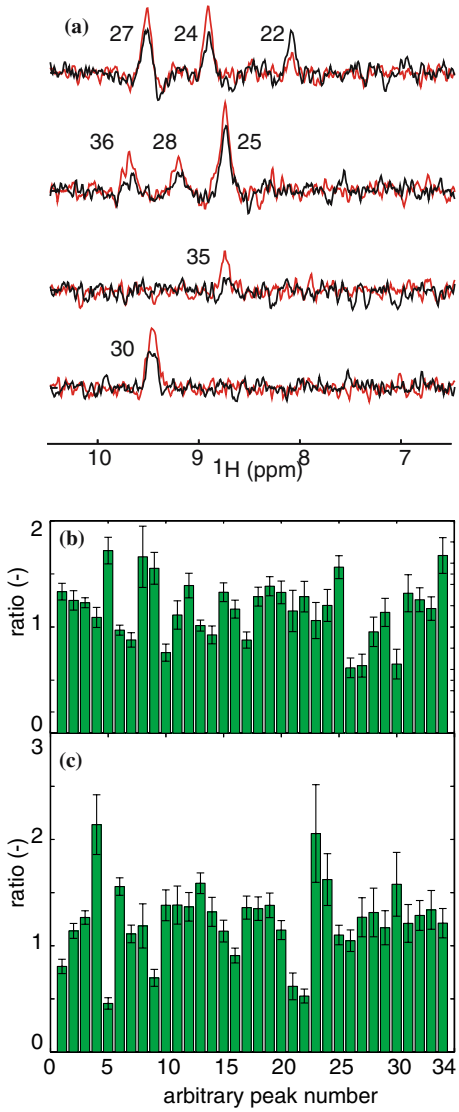

Figure 4. (a) slices extracted from the spectra of Figure 2d (red) and c (black). The corresponding peak numbers are indicated. (b) Ratio between the signal intensities of the TROPIC and the CRIPT experiments for T_T = 2.44 ms and T_C = 0.91 ms. (c) Same as (b) for T_T = 1.66 ms and T_C = 0.70 ms. Peak numbers are defined in Figure 2.

spectra as can also be observed in Figure 2. This is observed for 9 peaks (decreased on average by about 19% with a standard deviation of 14%) when T_C = 0.9 ms and T_T = 2.4 ms, and for 6 peaks (decreased on average by about 32% with a standard deviation of 17%) when T_C = 0.7 ms and T_T = 1.6 ms. This can be explained in part by pulse imperfections that will penalize the TROPIC experiment because of its many small flip angle pulses. This effect can be added to reductions in the optimal enhancement due to variations in the relaxation rates, as previously mentioned (see Figure 3). More importantly the preservation of water along the positive longitudinal axis is of prime importance in the current experiment. When a water presaturation scheme is used instead of water flip-back pulses, about 75% of the signal is lost in both experiments, in agreement with what is reported in Riek et al. (2002). Maintaining the water along the positive z-axis is harder to achieve in the TROPIC experiment with a number of small flip-back pulses. Moreover the water spends more time along the negative axis in the long TROPIC pulse sequence than in the shorter CRIPT experiment. In TROPIC with T_T = 1.6 ms, the 6 peaks that are reduced (peaks 1, 5, 9, 16, 21, and 22) all have lower frequencies than the others and are thus closer to the water frequency. Since this experiment requires many short flip-back pulses (due to the shorter delays τ_i), the less selective pulses affect signals with frequencies close to the water, as found in simulations. For sequences shorter than those utilized in the current work, it might be preferable to control the water trajectory by using only one pulse before the TROPIC transfer period and another pulse after this period. The length of the water selective pulse, which is limited by the delays τ_i, would otherwise correspond to a bandwidth that would affect amide proton frequencies. In spite of its more difficult experimental challenges, the TROPIC experiment has a significantly better sensitivity. The average enhancement is about 30% (calculated on 25 peaks) with a standard deviation of 19% for T_T = 2.4 ms and T_C = 0.9 ms, while an enhancement of 37% (calculated on 28 peaks) with a standard deviation of 25% was determined for the second pair of experiments. If one includes the peaks that are decreased, the overall enhancements are 19% and 25% for T_T = 2.4 ms and T_T = 1.6 ms, respectively. This is in agreement with the 21% expected theoretically, if one accounts for variations in the magnitudes and the ratio of the two relaxation rates involved in the transfer.

Conclusions

Using methods of optimal control theory, we were able to develop an experiment that enhances the sensitivity by 20–25% over the CRIPT method.

The TROPIC experiment was successfully implemented although only a crude estimation of the relaxation rates was used, and despite challenges related to water suppression. The technique has been shown to be more robust than CRIPT in presence of variations in relaxation rates, which maximizes the information content of the spectra. This practical demonstration of the principle of using optimal control theory for pulse sequence design opens the venue to a number of applications. For small molecules, optimal control theory can be used to optimize INEPT transfers, or even a combination of cross-correlated and scalar coupling mediated transfers (Khaneja et al., 2004). For larger molecules, such as GroEL, we showed that the TROPIC pulse sequence becomes the technique of choice for cross-correlation driven transfers – provided that the water is carefully maintained longitudinal during the experiment. Furthermore these methods of optimally manipulating dynamics of quantum mechanical systems in presence of decoherence are expected to have applications in the whole field of coherent spectroscopy and quantum information.

Supporting material available in electronic form (at http://dx.doi.org/10.1007/s10858-005-3592-0): Dynamic programming method for finding optimal flip angles and delays for the TROPIC pulse sequence.

Acknowledgements

We thank Dr Dmitri Ivanov for useful discussions. This research was supported by grants from NIH (GM 47467 and RR00995 to GW) and NSF (NSF 0133673 and AFOSR FA9550-04-1-0427 to NK). SJG acknowledges support from the Deutsche Forschungsgemeinschaft (Gl 203/4-2).

References

Abelson, J.N. and Simon, M.I. (2001) In *Methods in Enzymology Vol. 338. Nuclear Magnetic Resonance of Biological Macromolecules*, James, T.L., Doetsch, V. and Schmitz, U. (Eds.), Academic Press, San Diego.

Bax, A. and Cornilescu, G. (2000) *J. Am. Chem. Soc.*, **122**, 10143–10154.

Bodenhausen, G. and Ruben, D.J. (1980) *Chem. Phys. Lett.*, **69**, 185–189.

Boyd, J. Hommel, U. and Krishnan, V.V. (1991) *Chem. Phys. Lett.*, **187**, 317–324.

Brüschweiler, R. and Ernst, R.R. (1991) *J. Chem. Phys.*, **96**, 1758–1766.

Brüschweiler, R. Liao, X. and Wright, P.E. (1995) *Science*, **268**, 886–889.

Brutscher, B. Skrynnikov, N.R. Bremi, T. Brüschweiler, R. and Ernst, R.R. (1998) *J. Magn. Reson.*, **130**, 346–351.

Cavanagh, J. Fairbrother, W.J. Palmer, A.G. and Skelton, N.J. (1996) *Protein NMR Spectroscopy Principles and Practice,* Academic Press, San Diego.

Dalvit, C. (1992) *J. Magn. Reson.*, **97**, 645–650.

Ferentz, A.E. and Wagner, G. (2000) *Q. Rev. Biophys.*, **33**, 29–65.

Fischer, M.W.F. Zeng, L. Pang, Y. Hu, W. Majumdar, A. and Zuiderweg, E.R.P. (1997) *J. Am. Chem. Soc.*, **119**, 12629–12642.

Frueh, D. (2002) *Progr. NMR Spectrosc.*, **41**, 305–324.

Goldman, M. (1984) *J. Magn. Reson.*, **60**, 437–452.

Grzesiek, S. and Bax, A. (1993) *J. Am. Chem. Soc.*, **115**, 12593–12594.

Khaneja, N. Li, J.S. Kehlet, C. Luy, B. and Glaser, S.J. (2004) *Proc. Natl. Acad. Sci. USA*, **101**, 14742–14747.

Khaneja, N. Luy, B. and Glaser, S.J. (2003a) *Proc. Natl. Acad. Sci. USA*, **100**, 13162–13166.

Khaneja, N. Reiss, T. Luy, B. and Glaser, S.J. (2003b) *J. Magn. Reson.*, **162**, 311–319.

Lienin, S.F. Bremi, T. Brutscher, B. Brüschweiler, R. and Ernst, R.R. (1998) *J. Am. Chem. Soc.*, **120**, 9870–9879.

Nishihara, K. Kanemori, M. Yanagi, H. and Yura, T. (2000) *Appl. Environ. Microbiol.*, **66**, 884–889.

Pervushin, K. Riek, R. Wider, G. and Wüthrich, K. (1997) *Proc. Natl. Acad. Sci. USA*, **94**, 12366–12371.

Riek, R. Fiaux, J. Bertelsen, E.B. Horwich, A.L. and Wüthrich, K. (2002) *J. Am. Chem. Soc.*, **124**, 12144–12153.

Riek, R. Wider, G. Pervushin, K. and Wüthrich, K. (1999) *Proc. Natl. Acad. Sci. USA*, **96**, 4918–4923.

Woessner, D.E. (1962) *J. Chem. Phys.*, **37**, 647.